Identification of 10 differentially expressed genes involved in the tumorigenesis of cervical cancer *via* next-generation sequencing

Jia Xu[1,2], Wen Yang[2], Xiufeng Xie[2], Chenglei Gu[2], Luyang Zhao[2], Feng Liu[2], Nina Zhang[2], Yuge Bai[2], Dan Liu[2], Hainan Liu[2], Xiangshu Jin[2] and Yuanguang Meng[1,2]

[1] School of Medicine, Nankai University, Tianjin, China
[2] Department of Obstetrics and Gynecology, The Seventh Medical Center of Chinese PLA General Hospital, Beijing, China

ABSTRACT

Background: The incidence and mortality of cervical cancer remain high in female malignant tumors worldwide. There is still a lack of diagnostic and prognostic markers for cervical carcinoma. This study aimed to screen differentially expressed genes (DEGs) between normal and cervical cancer tissues to identify candidate genes for further research.

Methods: Uterine cervical specimens were resected from our clinical patients after radical hysterectomy. Three patients' transcriptomic datasets were built by the next generation sequencing (NGS) results. DEGs were selected through the edgeR and DESeq2 packages in the R environment. Functional enrichment analysis, including GO/DisGeNET/KEGG/Reactome enrichment analysis, was performed. Normal and cervical cancer tissue data from the public databases TCGA and GTEx were collected to compare the expression levels of 10 selected DEGs in tumor and normal tissues. ROC curve and survival analysis were performed to compare the diagnostic and prognostic values of each gene. The expression levels of candidate genes were verified in 15 paired clinical specimens *via* quantitative real-time polymerase chain reaction.

Results: There were 875 up-regulated and 1,482 down-regulated genes in cervical cancer samples compared with the paired adjacent normal cervical tissues according to the NGS analysis. The top 10 DEGs included *APOD*, *MASP1*, *ACKR1*, *C1QTNF7*, *SFRP4*, *HSPB6*, *GSTM5*, *IGFBP6*, *F10* and *DCN*. GO, DisGeNET and Reactome analyses revealed that the DEGs were related to extracellular matrix and angiogenesis which might influence tumorigenesis. KEGG enrichment showed that PI3K-Akt signaling pathway might be involved in cervical cancer tumorigenesis and progression. The expression levels of selected genes were decreased in tumors in both the public database and our experimental clinical specimens. All the candidate genes showed excellent diagnostic value, and the AUC values exceeded 0.90. Additionally, *APOD*, *ACKR1* and *SFRP4* expression levels could help predict the prognosis of patients with cervical cancer.

Conclusions: In this study, we selected the top 10 DEGs which were down-regulated in cervical cancer tissues. All of them had dramatically diagnostic value. *APOD*, *ACKR1* and *SFRP4* were associated with the survivals of cervical cancer. *C1QTNF7*,

HSPB6, *GSTM5*, *IGFBP6* and *F10* were first reported to be candidate genes of cervical carcinoma.

INTRODUCTION

Cervical cancer is the fourth most frequently diagnosed malignant tumor in women worldwide, and it caused approximately 348,189 deaths in 2022 (*Bray et al., 2024*). It is one of the leading causes of death in regions such as Africa, Melanesia, South Central Asia and South Eastern Asia (*Bray et al., 2024*). Even in developed countries such as the USA, it is still estimated that there were 13,960 new cases and 4,310 deaths in 2023 (*Siegel et al., 2023*). High-risk human papillomavirus (HR-HPV) infection is the main pathogenic factor of cervical cancer. Other risk factors include smoking, immunosuppression, early sexual life, long-term use of oral contraceptives, a higher number of childbirths and so on (*Bedell et al., 2020*; *Nagelhout et al., 2021*). Generally, the early-stage cervical cancer patients can achieve a 4.5-year survival rate of 99.2% for open surgery and 99.0% for minimally invasive surgery (*Salvo et al., 2022*). However, the advanced and recurrent cervical cancer patients usually have poor prognoses.

The mechanism of the malignant transformation of cervical epithelial cells has not been clearly elucidated. When HR-HPV infect cervical epithelial cells and accomplish genomic integration, the E6 and E7 proteins derived from HPV inactivate the tumor suppressor genes p53 and pRb, respectively (*Narisawa-Saito & Kiyono, 2007*). Some major molecular pathways are involved in the deteriorative progression, including RAF/MEK/ERK, PI3K/AKT, EGFR/VEGFR, Wnt/β-catenin, apoptosis (such as Bcl-2 sub-family) and coupled membrane receptor signaling (*Manzo-Merino et al., 2014*). The interfering processes of cell proliferation, apoptosis, cell migration, cell invasion and angiogenesis contribute to the formation of cervical cancer. Besides, immune escape is another important factor of cervical cancer incidence (*Kusakabe et al., 2023*). It is reported that the inhibition of NF-κB, STAT1, IRF3, IRF1, MIP-3α and HLA class I resulted in the carcinogenesis of cervical cancer (*Kusakabe et al., 2023*). *Volkova, Pashov & Omelchuk (2021)* summarized cervical cancer biomarkers grouped by different tumorigenesis pathways. E6/E7 mRNA, p16INK4a and serum SCC-Ag were representative in clinical practice among them.

Following the rise of cervical cancer screening tests and HPV vaccines, the awareness of preventing cervical cancer has gradually strengthened in recent years. Since 2018, the WHO has set goals for elimination of cervical cancer worldwide. It is of vital importance to find sensitive and specific biomarkers to guide the diagnosis and prognosis of cervical cancer.

In this study, we aimed to screen significant DEGs between cervical cancer tissues and paired adjacent normal cervical tissues based on RNA sequencing data. Public transcriptomic data from The Cancer Genome Atlas Program (TCGA) and the

Genotype-Tissue Expression Project (GTEx) were also taken into consideration to support our results. Meanwhile, we also performed confirmatory experiments to analyze the expression levels of the top 10 selected DEGs in another 15 pairs of normal and cervical cancer tissues, which included *Apolipoprotein D (APOD)*, *Mannose-Binding Lectin-Associated Serine Protease 1 (MASP1)*, *Atypical Chemokine Receptor 1 (ACKR1)*, *Complement C1q Tumor Necrosis Factor-Related Protein 7 (C1QTNF7)*, *Secreted Frizzled Related Protein 4 (SFRP4)*, *Heat Shock Protein Family B (Small) Member 6 (HSPB6)*, *Glutathione S-Transferase Mu 5 (GSTM5)*, *Insulin Like Growth Factor Binding Protein 6 (IGFBP6)*, *Coagulation Factor X (F10)* and *Decorin (DCN)*. These findings may provide novel candidate genes for diagnosis and prognosis of cervical cancer.

MATERIALS AND METHODS

Uterine cervical specimens

Uterine cervical specimens were separated immediately from the cervix of 18 cervical cancer patients after radical hysterectomy. The distance between cancer sample location and normal sample location was at least 2 cm. The patients were selected following the criteria below. Inclusion criteria: (1) Those who were eligible for this study and signed the informed consent; (2) Women aged 18–75 years; (3) Preoperative stage was IB1-IIA2, and surgery was the best treatment choice for them; (4) Those who had macroscopic cervical cancer tissues and adjacent normal tissues; (5) Those who were able to cooperate according to the research protocol. Exclusion criteria: (1) Pregnant or lactating women; (2) Preoperative stage was IIB or severe, and the preferred treatment was radiotherapy or chemotherapy; (3) Those whose cervical cancer tissues and adjacent normal tissues from the isolated uterine could not be distinguished; (4) Patients with severe circulatory, immune, or respiratory diseases; (5) Those who had other uncontrolled medical conditions that the researchers deem unsuitable for enrollment; (6) Any situation that the investigators considered may increase the risk to the subject or interfere with the results. Clinical information of the three patients whose specimens were used for RNA sequencing is shown in Table 1. Table 2 exhibited the key medical records of other 15 cases whose specimens were used for confirmatory experiments. The disease status was assigned according to the 2018 FIGO classification. Paired adjacent normal tissues and cancer tissues were stored long-term at −80 °C without any additive for subsequent experiments. The study was conducted in accordance with the principles of the Declaration of Helsinki. All the specimens were obtained after approval from the Ethics Committee of Seventh Medical Center of Chinese PLA General Hospital (S2023-025-01) and written informed consent was obtained from patients in the Department of Obstetrics and Gynecology of the Seventh Medical Center of PLA General Hospital.

RNA sequencing dataset establishment

Total RNA of paired adjacent normal tissues and cancer tissues from three patients was extracted by Trizol (Invitrogen, Waltham, MA, USA) according to the manufacturer's protocol. Therefore, we had three biological replicates. Three technical replicates were completed simultaneously. The extracted RNA of each sample was sequenced three times.

Table 1 Clinical information of three cervical cancer patients using in RNA sequencing.

	Age	HR-HPV type	Pathology	Stage	Operation	Neoadjuvant therapy	Postoperative therapy
Patient 1	35	16	Squamous cell carcinoma	IIA2	Robot-assisted laparoscopic radical hysterectomy + bilateral salpingectomy + pelvic lymph node resection	N/A	Concurrent chemoradiotherapy
Patient 2	61	16	Squamous cell carcinoma	IIA1	Laparoscopic radical hysterectomy + bilateral salpingectomy + pelvic lymph node resection	N/A	N/A
Patient 3	46	16	Squamous cell carcinoma	IB2	Laparoscopic radical hysterectomy + bilateral adnexectomy + pelvic lymph node resection	N/A	Concurrent chemoradiotherapy

Total amounts and integrity of RNA were assessed using the RNA Nano 6000 Assay Kit of the Bioanalyzer 2100 system (Agilent Technologies, Santa Clara, CA, USA). Then, total RNA was used as input material for the library preparation. Messenger RNA was purified from total RNA by using poly-T oligo-attached magnetic beads. After the construction of the library, the library was initially quantified by Qubit2.0 Fluorometer (Thermo Fisher Scientific Inc., Waltham, MA, USA), then diluted to 1.5 ng/μl, and the insert size of the library was detected by Agilent 2100 bioanalyzer. After insert size met the expectation, RT-qPCR was used to accurately quantify the effective concentration of the library (the effective concentration of the library is higher than that of 2 nM) to ensure the quality of the library. After the library was qualified, the different libraries were pooled according to the effective concentration and the target amount of data off the machine, then sequenced by the Illumina NovaSeq 6000 (Illumina, San Diego, CA, USA) (Fig. 1A). The end reading of 150 bp pairing is generated. Illumina Casava1.8 software (Illumina, San Diego, CA, USA) was used for basecalling. The basic principle of sequencing is to synthesize and sequence at the same time (Sequencing by Synthesis). After quality control for the reads, index of the reference genome (hg38) was built using Hisat2 (v2.0.5) and paired-end clean reads were aligned to the reference genome using Hisat2 (v2.0.5). FeatureCounts (v1.5.0-p3) was used to count the reads numbers mapped to each gene. The process of building RNA sequencing datasets was similar to what we described in our previous work (*Zhao et al., 2018*). Sequence data of this study have been deposited in the Gene Expression Omnibus (GEO) repository with the primary accession record GSE253690. The sequencing depth is 35.099995, and the statistical power of this experimental design calculated in R environment is 0.140838.

Identification of DEGs and functional enrichment analysis

Differential expression analysis of two groups (paired adjacent normal cervical tissues and cervical cancer tissues) of three patients was performed respectively using the edgeR package (Version 3.22.5) in the R environment (Version 4.2.1) as described in *Robinson, McCarthy & Smyth (2010)*. The integrated DEGs union between normal group and cancer group of all three patients were analyzed using the DESeq2 package (Version 1.20.0) following the method in *Love, Huber & Anders (2014)* and shown in Volcano diagram. The resulting p-values were adjusted using the Benjamini and Hochberg's approach for

Table 2 Clinical information of 15 cervical cancer cases using in quantitative real-time PCR.

	Age	HR-HPV type	Pathology	Molecular marker	Stage	Operation	Neoadjuvant therapy	Postoperative therapy
Case 1	44	16	Squamous cell carcinoma	p16 (+), p40 (+), Ki-67 (+), p53 (+), CK5/6 (+), EGFR (+), PD-L1 (CPS = 10)	IB3	Robotic-assisted laparoscopic radical hysterectomy + bilateral salpingectomy + pelvic lymph node resection	Chemotherapy	Concurrent chemoradiotherapy
Case 2	52	16	Squamous cell carcinoma	Ki-67 (+50%), p16 (+), p53 (+10%, mutant), CK5/6 (+), p40 (+), HER-2 (−), PD-L1 (CPS = 3), EGFR (+)	IB3	Laparoscopic radical hysterectomy + bilateral adnexectomy + pelvic lymph node resection	N/A	Concurrent chemoradiotherapy
Case 3	63	16	Squamous cell carcinoma	Ki-67 (+), p16 (+), p53 (+, wildtype), CK5/6 (+), p40 (+), HER-2 (1+), PD-L1 (CPS = 6)	IIIC2 (p)	Robotic-assisted laparoscopic radical hysterectomy + bilateral adnexectomy + para-aortic and pelvic lymph node resection	N/A	Concurrent chemoradiotherapy
Case 4	64	18	Adenosquamous carcinoma	p16 (+), p63 (+), p40 (+), PR (+), p53 (+, wildtype), PAX-2 (−), PTEN (−), Ki-67 (+), EGFR (+)	IIA1	Robotic-assisted laparoscopic radical hysterectomy + bilateral adnexectomy + pelvic lymph node resection	N/A	N/A
Case 5	39	18	Adenocarcinoma	p53 (+, wildtype), p16 (+), CD5/6 (+), p63 (−), CK7 (+), CK8/18 (+), CEA (−), PR (−), AB-PAS (+), p40 (+), PD-L1 (TC = 70%), EGFR (+), Ki-67 (+)	IIIC1 (r)	Robotic-assisted laparoscopic radical hysterectomy + bilateral adnexectomy + para-aortic and pelvic lymph node resection (patient request)	Chemotherapy	Concurrent chemoradiotherapy
Case 6	46	18	Adenosquamous carcinoma, focal cell neuroendocrine carcinoma	AE1/AE3 (+), Vimentin(−), p16 (+), CEA (+), CK7 (+), CK5/6 (−), p40 (−), Syn (NEC+), CgA (−), Ki-67 (+), PR (−), CD10 (−), AB-PAS (+), PD-L1 (CPS < 1)	IB3	Robotic-assisted laparoscopic radical hysterectomy + bilateral adnexectomy + para-aortic and pelvic lymph node resection	N/A	Radiotherapy
Case 7	68	N/A	Adenosquamous carcinoma	p16 (+), CK5/6 (+), CK7 (+), p63 (+), CD117 (+), Ki-67 (+), p53(+), SMA (−), Calponin (−), Syn (−), CD56 (+)	IIA1	Laparoscopic radical hysterectomy + bilateral adnexectomy + pelvic lymph node resection	N/A	Chemotherapy

(Continued)

Table 2 (continued)

|	Age	HR-HPV type	Pathology	Molecular marker	Stage	Operation	Neoadjuvant therapy	Postoperative therapy
Case 8	59	16	Squamous cell carcinoma	p16 (+), S-100 (−)	IIA1	Laparoscopic radical hysterectomy + bilateral adnexectomy + para-aortic and pelvic lymph node resection	N/A	Concurrent chemoradiotherapy
Case 9	46	16	Squamous cell carcinoma	CK7 (+), p40 (+), Ki-67 (+), PD-L1 (CPS < 1), p53 (+, wildtype), p16 (+)	IB2	Laparoscopic radical hysterectomy + bilateral adnexectomy + pelvic lymph node resection	N/A	Concurrent chemoradiotherapy
Case 10	47	16	Squamous cell carcinoma	Ki-67 (+), p16 (+), p53 (+), CK5/6 (+), p40 (+)	IB2	Laparoscopic radical hysterectomy + bilateral adnexectomy + pelvic lymph node resection	N/A	Radiotherapy
Case 11	61	16	Squamous cell carcinoma	p40 (+), p16 (+), p63 (+), Ki-67 (+), PD-L1 (CPS = 40)	IIA1	Laparoscopic radical hysterectomy + bilateral adnexectomy + pelvic lymph node resection	N/A	N/A
Case 12	36	N/A	Squamous cell carcinoma	Ki-67 (+), p16 (+), p53 (+, wildtype), CK5/6 (+), CK7 (+), CAM5.2 (+), CEA (+)	IIA1	Laparoscopic radical hysterectomy + bilateral salpingectomy + para-aortic and pelvic lymph node resection	N/A	Concurrent chemoradiotherapy
Case 13	42	16/58	Gastric adenocarcinoma	PAX-8 (+), CK7 (+), ER (−), PR (−), CK20 (−), SATB2 (−), Ki-67 (+), p16 (−), MUC6 (+), MUC5AC (+), PD-L1 (CPS = 15), AB (+), PAS (+)	IB2	Laparoscopic radical hysterectomy + bilateral adnexectomy + pelvic lymph node resection	N/A	Chemotherapy
Case 14	30	18	Adenosquamous carcinoma	p16 (+), Ki-67 (+), p53 (+, wildtype), CK5/6 (+), p63 (+), CK7 (+), CK8/18 (+), PD-L1 (CPS = 90), p40 (+)	IB1	Laparoscopic radical hysterectomy + bilateral salpingectomy + pelvic lymph node resection	N/A	N/A
Case 15	44	16	Squamous cell carcinoma	p16 (+), Ki-67 (+), PD-L1 (CPS = 5), p53 (+, wildtype)	IB2	Laparoscopic radical hysterectomy + bilateral salpingectomy + para-aortic and pelvic lymph node resection	N/A	N/A
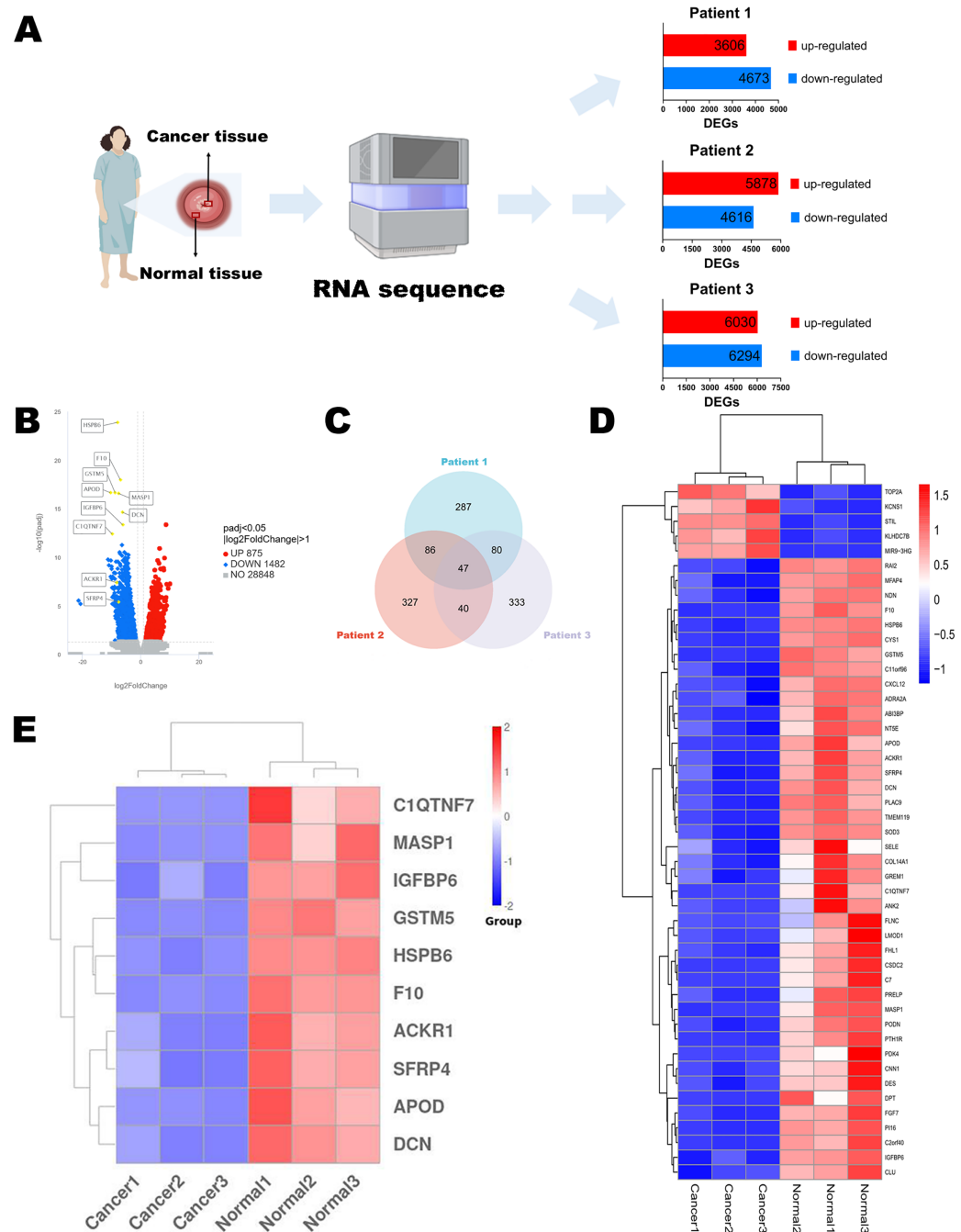
Figure 1 Identification of DEGs. (A) Flow chart of RNA sequencing. (B) Volcano diagram of DEGs in RNA sequencing results of three paired normal and cervical cancer samples. (C) Venn diagram of the top 500 DEGs of each pair of normal and cervical cancer samples. (D) Heatmap of the 47 intersecting DEGs. (E) Heatmap of the top 10 genes in 47 DEGs. Statistical methods were Shapiro-Wilk normality test and Levene's test. Figure 1A was created with BioRender.com. Full-size ☒ DOI: 10.7717/peerj.18157/fig-1

controlling the false discovery rate. We defined $padj \leq 0.05$ and $|\log_2(\text{foldchange})| \geq 1$ as the thresholds for significantly differential expression. We selected the top 500 DEGs of each patient through edgeR package. There were 47 intersecting genes in Venn diagram, and we selected the top 10 genes for next-step public data and experimental analysis. The

heatmap of 47 genes and 10 genes were plotted using pheatmap package and ggplot2 package (Version 3.3.6).

The integrated DEGs union of the 3 patients were used for enrichment analysis. Gene Ontology (GO) enrichment analysis was implemented by the clusterProfiler R package (Version 3.8.1), in which gene length bias was corrected. GO terms with corrected p values less than 0.05 were considered significantly enriched with DEGs. The Kyoto Encyclopedia of Genes and Genomes (KEGG) is a database resource for understanding high-level functions and utilities of the biological systems, especially large-scale molecular datasets generated by genome sequencing and other high throughput experimental technologies. We used clusterProfiler R package (Version 3.8.1) to test the statistical enrichment of DEGs in KEGG pathways. The Disease Gene Network (DisGeNET) database integrates human disease-related genes. DisGeNET pathways with corrected p values less than 0.05 were considered significantly enriched by DEGs. The Reactome database brings together the various reactions and biological pathways of human model species. Reactome pathways with corrected p values less than 0.05 were considered significantly enriched by DEGs. We also used clusterProfiler R package (Version 3.8.1) to test the statistical enrichment of DEGs in the Reactome pathway and the DisGeNET pathway. The functional enrichment analysis was performed as previously described in *Yu et al. (2012)*.

Public RNA sequencing data analysis

Public data (RNA sequencing data and clinical information) were requested from TCGA and GTEx databases provided on the UCSC Xena website (http://xenabrowser.net/datapages/). The FPKM-form RNA sequencing data were uniformly treated through Toil process (*Vivian et al., 2017*). The expression of selected DEGs was transformed into $\log_2$(FPKM+1) values to compare the differences. The receiver operating characteristic (ROC) curves were analyzed by pROC package (Version 1.18.0) which was described in *Robin et al. (2011)*. Diagnostic values were measured by area under the curve (AUC) values. Survival analysis was finished using overall survival (OS) time through survival package (Version 3.3.1) described in *Groeneveld et al. (2019)*. Survival outcomes referred to data from the literature reported in 2018 (*Liu et al., 2018*). The groups were divided by the median value of the expression level of each DEG.

Quantitative real time polymerase chain reaction

Total RNA was extracted from 20–30 mg paired adjacent normal cervical tissues and cervical cancer tissues through macrodissection according to the manufacturer's protocol of total RNA rapid extraction kit (BIOMAN, Beijing, China) within 1 week. All the equipments were purified with DEPC water. RNase free water was used for the dilution of RNA. The adsorption columns in the kit were used to remove DNA and purify RNA. The quality of RNA was assessed by the A260/A280 and A260/A230 value of each sample using Multiskan Skyhigh (Thermo Fisher Scientific, Waltham, MA, USA) and all the values were conformed to the standard. RNA (200 ng for each sample) was reverse-transcribed into cDNA by reverse transcriptase and random primer (N9) (0.1 μg/μl) in a 20 μl reaction volume with transcript one-step gDNA removal and cDNA synthesis supermix kit

(TRANSGEN, Beijing, China). The reverse-transcribed reaction conditions included 25 °C for 10 min, 42 °C for 15 min and 85 °C for 5 s. cDNA was stored at −20 °C and was used for qPCR within 1 week. RT-qPCR was performed using the PerfectStart Green qPCR Supermix kit (TRANSGEN, Beijing, China) in 0.2 mL Polypropylene PCR Tube Strips (Axygen, Union City, CA, USA) *via* QuantStudio 3 Real-Time PCR System (ABI, Loma Linda, CA, USA). QuantStudio Design & Analysis Software (ABI, Waltham, MA, USA) was used for manual reaction setup and analysis. The PCR conditions included a denaturing step at 94 °C for 30 s and 45 cycles of 94 °C for 5 s and 60 °C for 30 s for real time plate read. The melt curve stage included 95 °C for 15 s, 60 °C for 1 min and 95 °C for 1 s. The whole reaction volume was 20 μl, and the concentration of forward and reverse primers were 10 μM. SYBR Green I was the fluorescent dye applied in this assay. GAPDH was used for data normalization. The $2^{-\Delta\Delta Ct}$ value was regarded as the expression level of each gene. The RT-qPCR was performed in investigator's lab and repeated three times similar to what we described in our previous work (*Jin et al., 2019*). The results showed well repeatability. Each melt curve has only one peak and we found little outliers. Targeted gene information and specific primer sequences were described in Table S1. The manufacturer of oligonucleotides was Sangon (Shanghai, China).

Statistical analysis

RNA sequencing and public database data were conducted using the R environment (Version 4.2.1). *Padj* ≤ 0.05 and $|\log_2(\text{foldchange})| \geq 1$ were the thresholds for DEGs. Corrected *p* values < 0.05 were considered significantly enriched in function enrichment analysis. Quantitative data were analyzed using Shapiro-Wilk normality test and Levene's test. The expression level difference was calculated by Mann–Whitney U test using stats package (Version 4.2.1) and car package (Version 3.1-0). The ROC curves were analyzed by pROC package (Version 1.18.0). Cox proportional hazard model was tested and survival curves were matched through survival package (Version 3.3.1) using Kaplan-Meier methodology. Then the difference in OS of cervical cancer patients stratified by target gene expression level was tested by the Log-rank test. Data visualization was accomplished *via* survminer package and ggplot2 package (Version 3.3.6). The comparison of 10 DEGs expression between paired normal and cancer samples from clinical sampling in RT-qPCR was analyzed by paired *t* test and plotted in Graphpad Prism 9 (GRAPHPAD SOFTWARE, CA, USA). *p* < 0.05 was considered statistically significant.

RESULTS

Identification of DEGs

To discuss the potential mechanisms of cervical cancer tumorigenesis and identify the DEGs involved in these processes, we extracted the specimens from three patients (stage IB2 to IIA2) after the radical hysterectomy. Their clinical information was shown in Table 1. Then, RNA sequences were determined by NGS. The up-regulated and down-regulated DEGs were sorted out, respectively (Fig. 1A). According to the integrated NGS data of three patients, there were 875 up-regulated and 1,482 down-regulated genes in cervical cancer tissues compared to paired adjacent normal cervical tissues (Fig. 1B).

DEGs were reported only if the log-fold change was >1 and the adjusted p value was less than 0.05. We focused on the top 500 DEGs of each patient, and found that their intersection contained 47 DEGs (Fig. 1C). The heatmap demonstrated that only five DEGs expressions were increased in cancer specimens, while other 42 DEGs expressions were obviously decreased (Fig. 1D). We chose the top 10 significant DEGs in the 47 intersectional DEGs for further research (Fig. 1E) and we marked their locations in the integrated DEGs union between normal group and cancer group of three patients (Fig. 1B). These genes included *APOD*, *MASP1*, *ACKR1*, *C1QTNF7*, *SFRP4*, *HSPB6*, *GSTM5*, *IGFBP6*, *F10* and *DCN*. All of them expressed at lower levels in cervical cancer samples than in normal cervix cells.

Functional enrichment analysis of DEGs

Functional enrichment analysis revealed the potential mechanisms of the DEGs union between normal group and cancer group of three patients in the development of cervical cancer. GO analysis is associated with cellular component (CC), molecular function (MF) and biological process (BP). It was indicated that the incidence of malignant cervical tumor could be attributed to extracellular matrix, angiogenesis and circulatory system process (Fig. 2A). DisGeNET database contains a collection of genes associated with abundant human diseases. The results showed that 2357 DEGs (including 875 up-regulated DEGs and 1482 down-regulated DEGs) were more likely to generate tumor angiogenesis, systemic scleroderma and malignant neoplasm of thyroid (Fig. 2B). KEGG database reflected the reaction network of molecules and pathways of diseases. We found that PI3K-Akt signaling pathway, calcium signaling pathway, neuroactive ligand-receptor interaction, cell cycle and focal adhesion may participate in the occurrence and progression of cervical cancer (Fig. 2C). Changes in extracellular matrix organization and cell cycle checkpoints were the two most important processes associated with cervical tumors on the basis of Reactome database (Fig. 2D).

The expression levels of selected DEGs in public database

The TCGA program is the largest public database of cancer genetic information worldwide. The database provides multi-omics hereditary information of cancer patients. The GTEx project collected the sequencing data of healthy human donors. In this study, we focused only on the transcriptomic information of 10 selected DEGs to verify their expression levels in a larger population. All the selected genes (including *APOD*, *MASP1*, *ACKR1*, *C1QTNF7*, *SFRP4*, *HSPB6*, *GSTM5*, *IGFBP6*, *F10* and *DCN*) showed lower expression levels in cervical cancer samples, and these results were statistically significant (Figs. 3A–3J).

The diagnostic performance of selected DEGs in public database

To assess the performance of these selected DEGs as biomarkers, ROC curves were generated to measure the AUC values. All the AUC values exceeded 0.90, which meant that the selected DEGs have chances to function as excellent diagnostic biomarkers (Figs. 4A–4J). In particular, the AUC values of *MASP1*, *GSTM5* and *C1QTNF7* were 0.998, 0.998
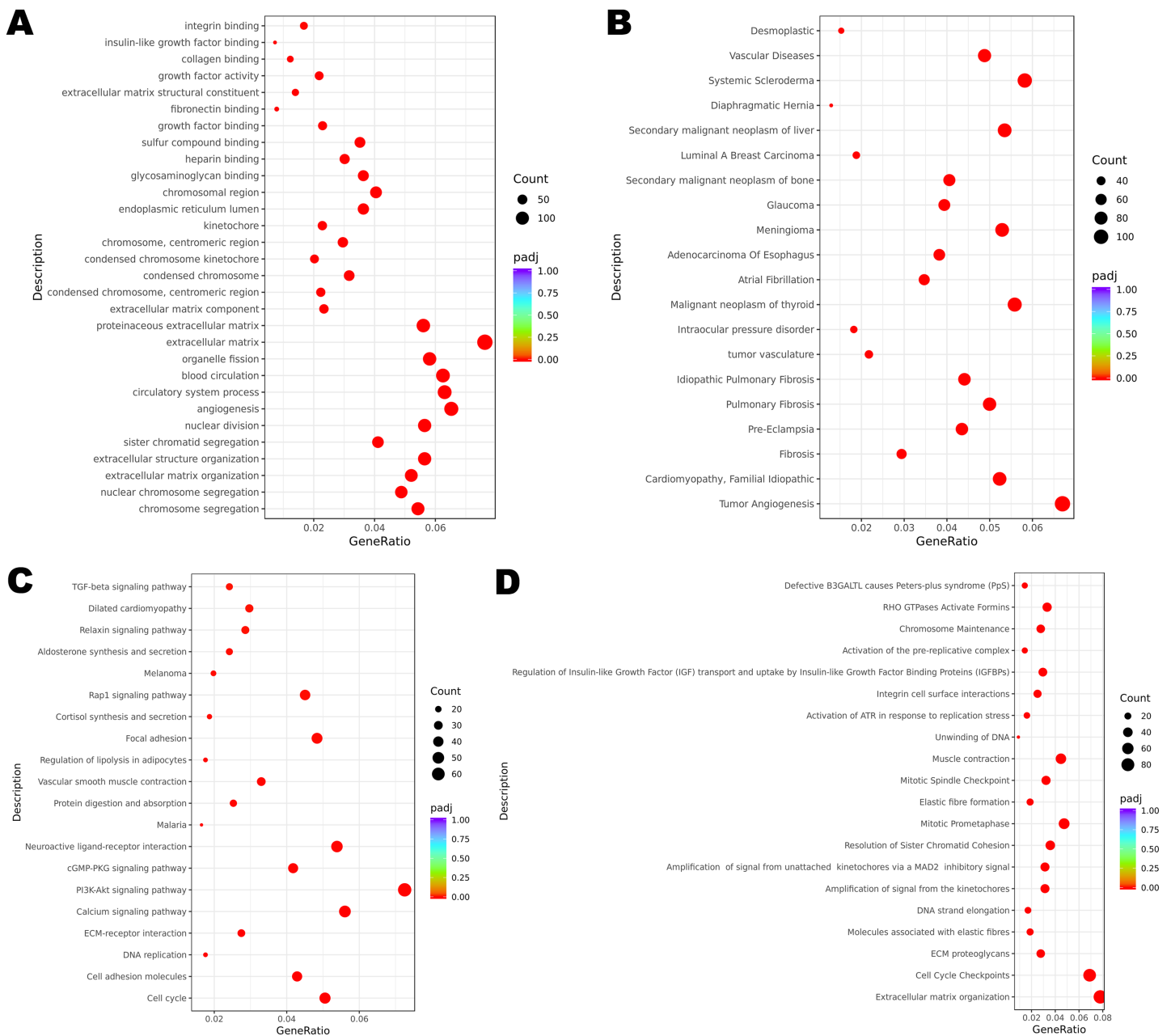
Figure 2 Functional enrichment of DEGs. (A) GO enrichment analysis of all the DEGs. (B) DisGeNET enrichment analysis of all the DEGs. (C) KEGG enrichment analysis of all the DEGs. (D) Reactome enrichment analysis of all the DEGs. Full-size ⬙ DOI: 10.7717/peerj.18157/fig-2

and 0.997, respectively (Figs. 4B, 4G, 4D). Other DEGs whose AUC values were greater than 0.99 included *APOD*, *HSPB6*, *F10* and *DCN* (Figs. 4A, 4F, 4I, 4J).

Survival analysis of selected DEGs in the TCGA program

Survival analysis was performed according to the OS time. The groups were divided by the median expression value of each target gene (Figs. 5A–5J). Only the expression levels of *APOD*, *ACKR1* and *SFRP4* contributed to the variation in OS. Patients who had
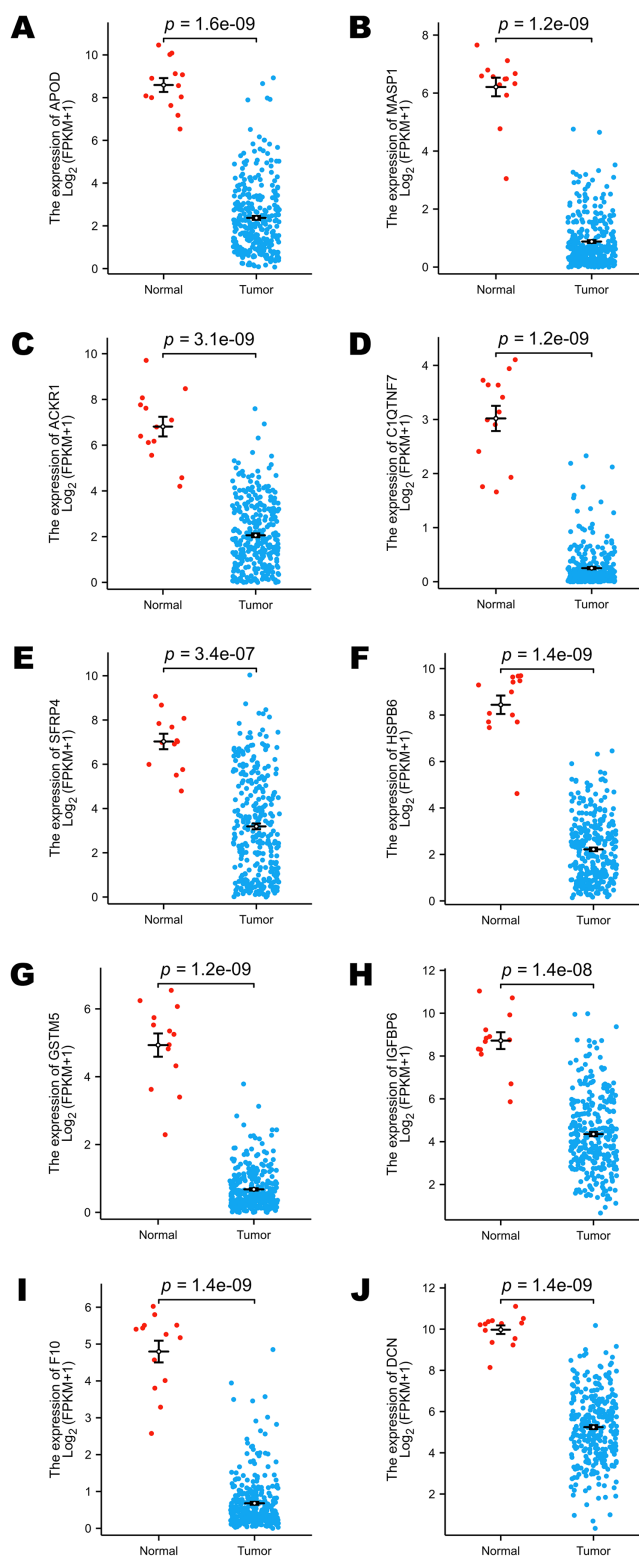
Figure 3 Comparison of the expression levels of selected DEGs between normal and cervical cancer samples in public databases. (A) Comparison of *APOD* expression levels in public databases. (B) Comparison of *MASP1* expression levels in public databases. (C) Comparison of *ACKR1* expression levels in public databases. (D) Comparison of *C1QTNF7* expression levels in public databases. (E) Comparison of *SFRP4* expression levels in public databases. (F) Comparison of *HSPB6* expression

Figure 3 (continued)

levels in public databases. (G) Comparison of *GSTM5* expression levels in public databases. (H) Comparison of *IGFBP6* expression levels in public databases. (I) Comparison of *F10* expression levels in public databases. (J) Comparison of *DCN* expression levels in public databases. Statistical method was Mann-Whitney U test. Data was presented as Mean ± SEM.   Full-size ◰ DOI: 10.7717/peerj.18157/fig-3
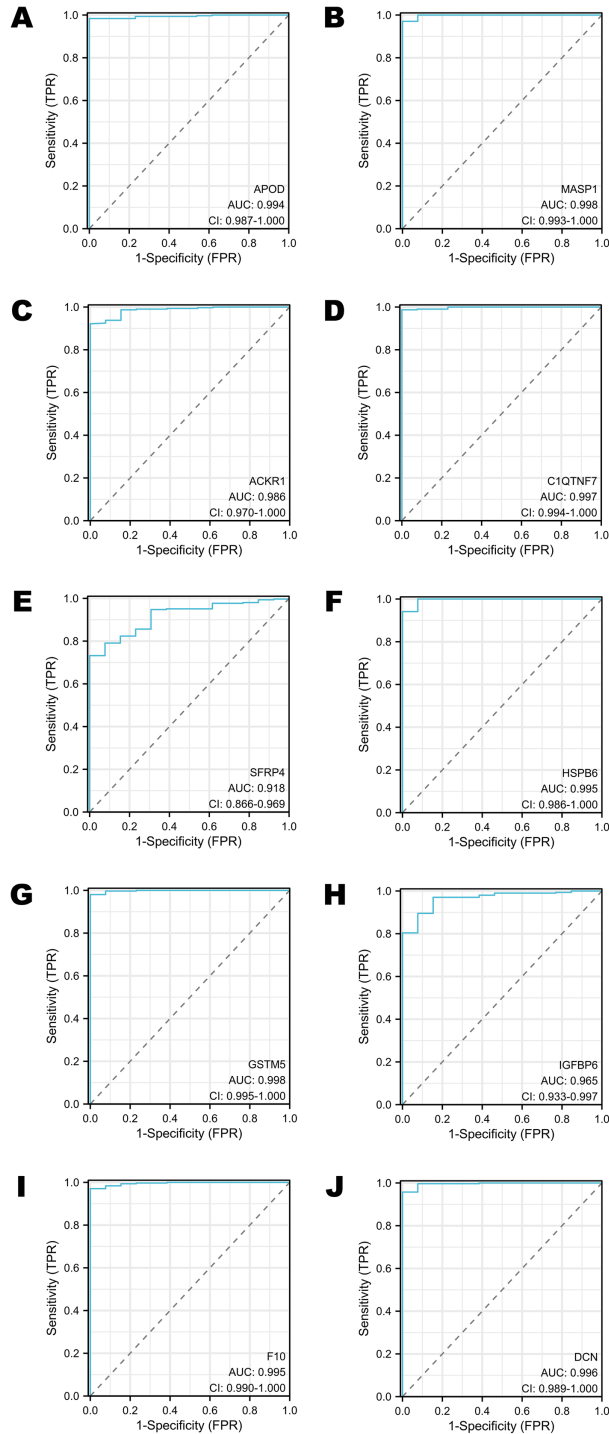
Figure 4 The ROC curves of selected DEGs in public databases. (A) The ROC curve of *APOD* in public databases. (B) The ROC curve of *MASP1* in public databases. (C) The ROC curve of *ACKR1* in

higher expression of *APOD*, *ACKR1* and *SFRP4* might have a longer survival time (Figs. 5A, 5C, 5E).

Selected DEGs were down-regulated in cervical cancer tissues

Fifteen pairs of cervical cancer tissues and adjacent normal cervical tissues were collected after the radical hysterectomy, and their brief clinical information were shown in Table 2. We performed RT-qPCR to determine the expressions of 10 selected DEGs in various patients (Figs. 6A–6J). *GAPDH* was used as the normalization gene. Similar to the analysis results of public database, the expression levels of most DEGs were down-regulated in cervical cancer tissues compared to the paired normal cervical tissues (Figs. 6A–6J). In Cases 2, 3, 8, 10, 11, 12 and 15, the expression levels of all 10 selected DEGs decreased significantly in cervical cancer tissues (Figs. S1B, S1C, S1H, S1J, S1K, S1L, S1O). The expression of *DCN* was almost unchanged in Case 5 (Fig. S1E), and *IGFBP6* expression remained stable in both normal and cancer tissues of Case 14 (Fig. S1N). However, the expression levels of other DEGs in Case 5 and 14 were lower in cancer tissues than that in normal tissues (Figs. S1E and S1N). All data in Fig. 6 and S1 showed that the expression levels of *APOD*, *MASP1*, *ACKR1* and *SFRP4* were extremely consistent in most cases, demonstrating that they have a potential to be biomarkers for cervical cancer diagnosis.

DISCUSSION

According to the RNA sequence of three patients, we chose the top 10 DEGs which included *APOD*, *MASP1*, *ACKR1*, *C1QTNF7*, *SFRP4*, *HSPB6*, *GSTM5*, *IGFBP6*, *F10* and *DCN* to compare the expression levels of normal and tumor tissues in public databases and our clinical specimens. The expression of 10 genes decreased significantly in most tumor samples. Moreover, we generated the ROC curves and performed survival analysis of selected genes. AUC values were greater for *APOD*, *MASP1*, *C1QTNF7*, *HSPB6*, *GSTM5*, *F10* and *DCN*. The higher expression levels of *APOD*, *ACKR1* and *SFRP4* are closely related to longer OS. The functional enrichment analysis of all the DEGs were accomplished. Extracellular matrix and angiogenesis were involved in the tumorigenesis process, while PI3K-Akt signaling pathway was the most remarkable potential mechanism.

The major biological functions of the 10 DEGs were various from literatures, and we summarized them in Table 3. Five of them have previously been associated with cervical cancer. APOD is a 25–30 kDa apolipoprotein whose biological functions were mostly associated with lipid metabolism and neuroprotection in the past, but it also had effects on lipid trafficking, food intake, inflammation, antioxidative response, development and even in different types of cancers (*Rassart et al., 2020*). Some research identified *APOD*, down-regulated in cervical tumor, as a DEG from public databases such as Gene Expression Profiling Interactive Analysis 2 (GEPIA2), and utilized *APOD* as one of the
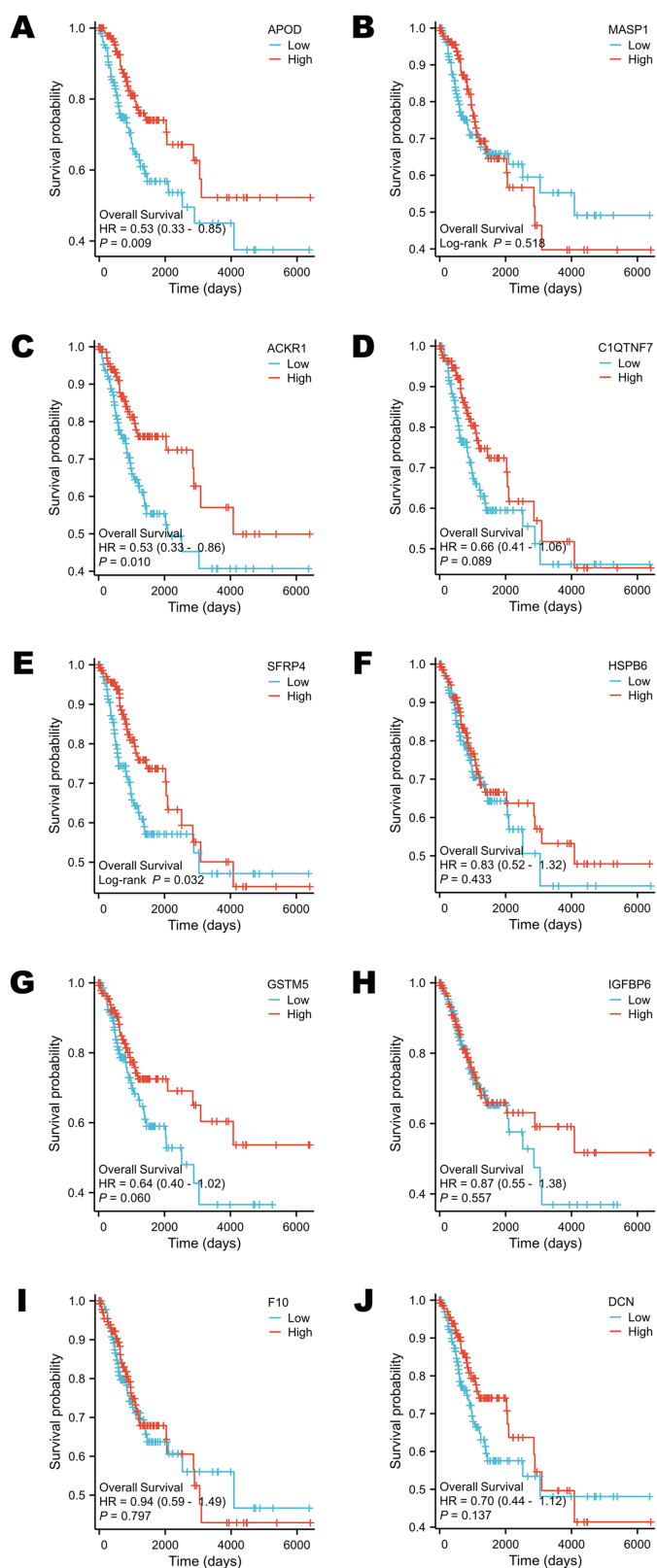
Figure 5 Survival analysis of selected DEGs in public database. (A) The survival analysis of *APOD* in public database. (B) The survival analysis of *MASP1* in public database. (C) The survival analysis of
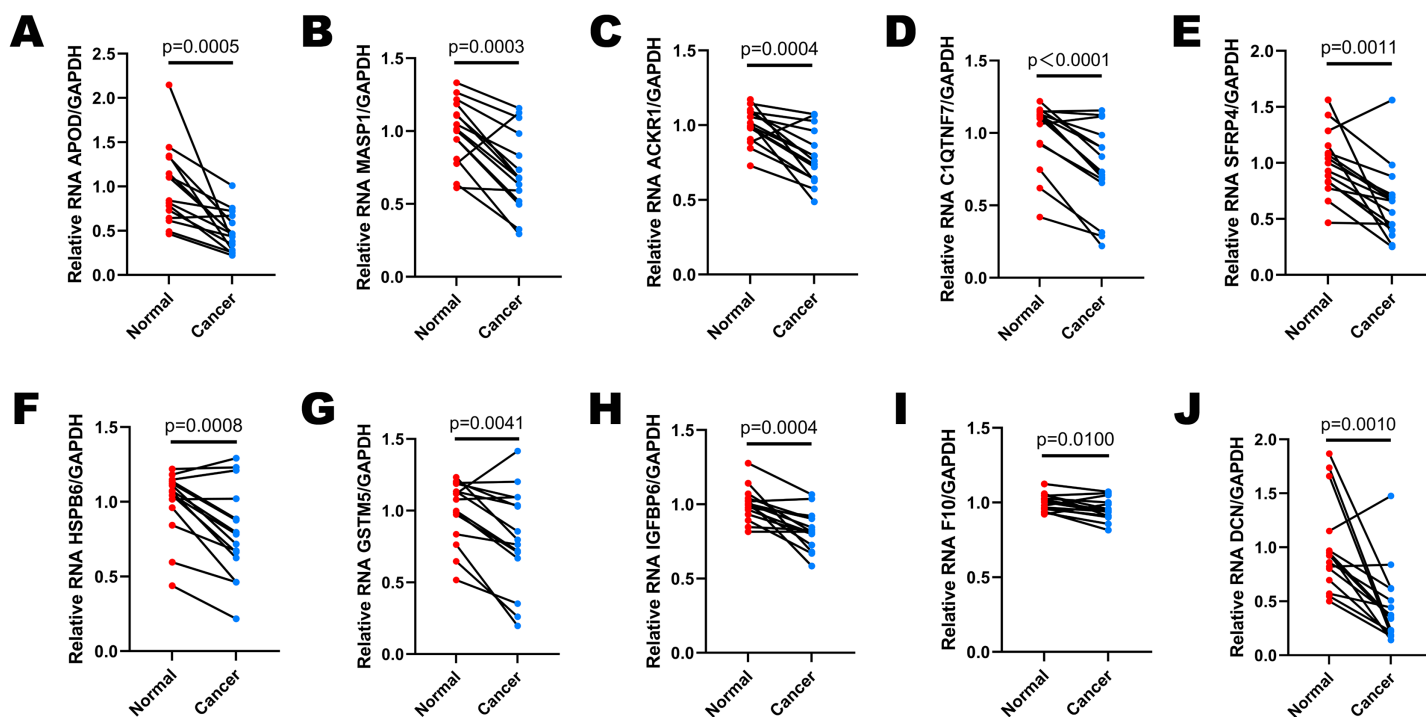
Figure 6 The expression levels of selected DEGs between paired adjacent normal cervical tissues and cervical cancer tissues by RT-qPCR. (A) The comparison of *APOD* expression between paired normal and cancer tissues. (B) The comparison of *MASP1* expression between paired normal and cancer tissues. (C) The comparison of *ACKR1* expression between paired normal and cancer tissues. (D) The comparison of *C1QTNF7* expression between paired normal and cancer tissues. (E) The comparison of *SFRP4* expression between paired normal and cancer tissues. (F) The comparison of *HSPB6* expression between paired normal and cancer tissues. (G) The comparison of *GSTM5* expression between paired normal and cancer tissues. (H) The comparison of *IGFBP6* expression between paired normal and cancer tissues. (I) The comparison of *F10* expression between paired normal and cancer tissues. (J) The comparison of *DCN* expression between paired normal and cancer tissues. Statistical method was paired *t* test. Data was presented as mean value of triplicates. Full-size ☑ DOI: 10.7717/peerj.18157/fig-6

biomarkers in prognostic model of cervical cancer (*Jiang et al., 2021*; *Wang et al., 2021*; *Zhang et al., 2022c*), which was consistent with our results. *Song et al. (2008)* even believed that *APOD* was a candidate gene involved in pathogenesis of invasion in cervical cancer since 2008. The above literatures approved our conclusion that APOD acts as a tumor suppressor in cervical cancer. MASP1 is one kind of the complexes of mannose-binding lectin and serine proteases and is able to activate C3 (*Matsushita, Endo & Fujita, 1998*). MASP1 could serve as a serum protein, so it was used to judge the prognosis of cervical cancer and response to chemotherapy (*Kong et al., 2020*; *Li et al., 2023*; *Maestri et al., 2018*). Since *MASP1* participated in the activities of complement system, we believed that future research on the influence of *MASP1* to immune escape of cervical cancer would be

valuable. *ACKR1*, also known as the *Duffy antigen receptor for chemokines (DARC)*, is a key regulator that binds chemokines involved in inflammatory responses, cancer proliferation, angiogenesis, and metastasis (*Crawford & Volkman, 2023*). *Hou et al. (2013)*, *Liu et al. (2020)* both linked the expression of *ACKR1* to lymph node metastasis and prognosis in cervical cancer, reaching a conclusion that ACKR1 might be a tumor suppressor. SFRP4 is a secreted protein with an affinity to bind to the Wnt ligands, participating in different developmental and adult homeostatic pathways (*Pawar & Rao, 2018*). The hypermethylation or decreased expression of *SFRP4* was supposed to have relationship with the occurrence and progression of cervical cancer, and antagonizing canonical Wnt signaling pathway through SFRP4 may become a new cancer therapy (*Chung et al., 2009*; *Ghoshal & Ghosh, 2016*; *Zhang, Chen & Shao, 2020*). *SFRP4* expression was also reduced in cervical cancer tissues in our experiments. Further research is needed on how SFRP4 functions on cervical cancer through Wnt/β-catenin signaling pathway. DCN, a leucine-rich extracellular matrix proteoglycan, is a suppressor of tumorigenesis, invasion and metastasis. It is said to be an essential regulatory factor in inflammation and ferroptosis (*Hu et al., 2021b*; *Liu et al., 2021*). *Wang et al. (2022a)* studied the relationship of long non-coding RNA (Lnc-RNA) PGM5-AS1 and cervical cancer, and finally discovered that the Lnc-RNA upregulated DCN to inhibit cervical cancer progression. Our GO enrichment analysis reported that extracellular matrix was intensively associated with cervical cancer development, and DCN may get involved in this process.

To our knowledge, the functions of other five genes were not reported in cervical cancer previously. *C1QTNF7*, also called *C1q complement/TNF related protein 7 (CTRP7)*, is an important target from adipokine family for metabolic syndrome, glucose tolerance, insulin sensitivity and vascular remodeling (*Bi et al., 2022*; *Hu et al., 2021a*; *Lata et al., 2022*; *Petersen et al., 2017*; *Wong et al., 2008*; *Xue et al., 2024*). It is also a secreted regulator of inflammation and cellular stress (*Petersen et al., 2017*). Besides, the increased expression of *C1QTNF7* in macrophages inhibited the proliferation and migration of trophoblasts, and further resulted in recurrent miscarriage (*Wang et al., 2022b*). It was predicted that the function of C1QTNF7 in metabolism, vascular remodeling and inflammation may affect the progression of cervical cancer. HSPB6 is a member of the family of heat shock proteins (HSP), which regulates the folding and degradation of proteins in cancer cell growth, proliferation, metastasis, and resistance to drugs (*Chen et al., 2021*; *Guo et al., 2023*; *Wu et al., 2023*; *Wyciszkiewicz et al., 2021*). It is also famous for its ability to provide cardioprotection (*Fan, Chu & Kranias, 2005*). The hypermethylation of *HSPB6* was observed in breast cancer and melanoma (*Edwards, Cameron & Baillie, 2011*; *Zhang et al., 2022b*). *HSPB6* phosphorylation showed anti-tumor activities in hepatocellular and prostate cancer cells (*Feng et al., 2024*; *Matsushima-Nishiwaki et al., 2016*). Besides, many researches linked the action of HSPB6 with enhanced apoptosis (*Feng et al., 2024*; *Guo et al., 2023*; *Ju et al., 2015*; *Nagasawa et al., 2014*; *Yang et al., 2022*). The role of HSPB6 in cervical cancer is still unclear. Our data showed *HSPB6* expression decreased in cervical cancer tissues, implying that it might participate in the progression of cervical cancer. The function of HSPB6 in cervical cancer progression needs further investigation. GSTM5 belongs to Glutathione S-transferase (GSTs) family, participating in cellular protection

Table 3 Major biological functions of 10 DEGs.

Gene	Gene description	Gene ID in ensembl	Major biological functions
APOD	Apolipoprotein D	ENSG00000189058	Lipid metabolism, lipid trafficking, neuroprotection, food intake, inflammation, antioxidative response, development, tumor behavior regulator
MASP1	Mannose-Binding Lectin-Associated Serine Protease 1	ENSG00000127241	Activate complements, participate in lectin activation pathway
ACKR1	Atypical Chemokine Receptor 1	ENSG00000213088	Chemokine receptor, inflammatory response, cancer proliferation regulator, cancer metastasis regulator, angiogenesis
C1QTNF7	Complement C1q Tumor Necrosis Factor-Related Protein 7	ENSG00000163145	A target from adipokine family, metabolic syndrome, glucose tolerance, vascular remodeling, regulator of inflammation and cellular stress
SFRP4	Secreted Frizzled Related Protein 4	ENSG00000106483	Regulator of Wnt/β-catenin signaling pathway, development, homeostatic establishment
HSPB6	Heat Shock Protein Family B (Small) Member 6	ENSG00000004776	Cardioprotection, regulatory factor of the folding and degradation of proteins in cancer cell growth, proliferation, metastasis, and resistance to drugs
GSTM5	Glutathione S-Transferase Mu 5	ENSG00000134201	Cellular protection from the environment and oxidative stress, detoxification modulator
IGFBP6	Insulin Like Growth Factor Binding Protein 6	ENSG00000167779	A relatively specific inhibitor of IGF-II, a regulator of DNA repair, ferroptosis and chemotaxis of immune cells
F10	Coagulation Factor X	ENSG00000126218	Coagulation, FX production, hematological system diseases, ability of anti-angiogenesis
DCN	Decorin	ENSG00000011465	Suppressor of tumorigenesis, suppressor of invasion and metastasis, regulatory factor in inflammation and ferroptosis

from the environment and oxidative stress (*Peng et al., 2008*). *Zhang et al. (2022a)* indicated that GSTM5 might reduce reactive oxygen species (ROS) level to ameliorate oxidative stress, and ultimately, regulate ovarian cancer stemness maintenance. Abnormal expression of GSTM5 was widely detected in malignant tumors such as gastric cancer, urothelial carcinoma and lung adenocarcinoma (*Chen et al., 2020*; *Hao et al., 2022*; *Jou et al., 2021*; *Shen et al., 2023*). We found that *GSTM5* expression was down-regulated in cervical cancer, which was valuable to discover the underlying mechanism. More attention might be paid on the potential influence of oxidative stress caused by reduced GSTM5 expression in cervical cancer. IGFBP6 is a relatively specific inhibitor of IGF-II, which means it also inhibits IGF II-induced proliferation, differentiation, migration and survival (*Bach Leon, Fu & Yang, 2012*). *Bach (2015b)* reviewed literatures and found that *IGFBP-6* expression was lower in malignant cells than in normal cells, which implied that it is an inhibitor of tumorigenic processes. Likewise, we found the same variation tendency in malignant cervical tissues and normal tissues. Reduced expression of *IGFBP6* could be used to identify breast, prostate, hepatocellular and colorectal cancer (*Bach, 2015a*; *Nikulin et al., 2021*; *Zhao et al., 2020*). It is also regarded as a regulator and prognostic factor for glioma (*Bei et al., 2016*). Wnt/β-catenin and Hedgehog signaling pathway regulated the expression of IGFBP6 (*Bach, 2015a*). Other potential biological changes caused by IGFBP6 contained DNA repair, ferroptosis and chemotaxis of immune cells (*Chua et al., 2015*;

Liso et al., 2018; *Nikulin et al., 2023*), which may induce cervical cancer to a certain extent. Coagulation processes interact with tumorigenesis and malignant behaviors (*Falanga, Marchetti & Vignoli, 2013*). Zymogen FX, encoded by *F10*, was reported to have the ability of anti-angiogenesis depending on the Gla domain (*Lange et al., 2014*). *Borensztajn et al. (2009)* and *Borensztajn, Peppelenbosch & Spek (2010)* confirmed that F10 specifically inhibits the migration of several cancer cell lines (breast, lung and colon cancer cells) dependent on protease-activated receptor-1 (PAR-1) signaling and LIM Domain Kinase (LIMK) activation. Additionally, *Graf et al. (2019)* found that rivaroxaban, an inhibitor of F10, promotes antitumor immunity. Since F10 influenced angiogenesis and migration, it is meaningful to explore whether cervical cancer had a relationship with coagulation changes.

It is also interesting to verify the diagnostic and prognostic value of the 10 DEGs using the public data. ROC curve is a plot that evaluated the accuracy of a diagnostic test or prognostic model. The x-axis and y-axis were used to describe (1-specificity) and sensitivity, respectively. Each point on ROC curve was confirmed under different cut-off value. The index we paid much attention to is the AUC value. The AUC value is between 0.5 and 1. A test that perfectly discriminated between two conditions such as health and tumor has an AUC close to 1.0 (*Alemayehu & Zou, 2012*; *Obuchowski & Bullen, 2018*). In this study, the AUC values of all these 10 DEGs were over 0.90, indicating that they had dramatic diagnostic value to identify cervical cancer, especially *MASP1*, *GSTM5* and *C1QTNF7*. Survival analysis reflects the survival status of different classification conditions over time (*Flynn, 2012*). It could be used to compare the follow-up of different groups of patients. Median expression level of each DEG was regarded as the classification standard in this research. Only the expression levels of *APOD*, *ACKR1* and *SFRP4* had influences on the OS of cervical cancer patients. These findings indicated that *APOD*, *ACKR1* and *SFRP4* may have the ability to predict survival outcomes. These genes could be regarded as prognostic biomarkers. All these novel biomarkers were likely to participate in the machine-learning diagnostic or prognostic models in the future.

All the expression levels of the 10 DEGs decreased significantly in most cases in our experiments, which was consistent with the results of public database analysis. Some of the 10 genes exhibited opposite results in different cases such as *MASP1* and *ACKR1* in case 9 (Fig. S1I). These results could be attributed to individual difference, for the selected genes participated in diverse biological process. Only *APOD*, *MASP1*, *ACKR1*, *SFRP4* and *DCN* have been reported in cervical cancer in previous studies, but all the related researches were only bioinformatics analysis or expression levels associated with clinical status. There is a lack of explanation of mechanism by which these genes influence the progression of cervical cancer. The correlation of cervical cancer with DEGs such as *C1QTNF7*, *HSPB6*, *GSTM5*, *IGFBP6* and *F10* is still unknown.

The limitation of our study was that we only analyzed the RNA sequencing results of three patients, resulting in a small sample size. Public database was included in the research to support these ideas, but the number of normal cervical samples was still limited. Fortunately, the 15 paired clinical specimens also reached a similar conclusion. In addition,

the mechanism of selected DEGs has not been explained distinctly in literature. Biological functional experiments should be completed in further studies.

CONCLUSIONS

Cervical malignant tumors seriously harm women's health. The diagnostic and prognostic biomarkers that have good sensitivity and specificity have not been explored until now. In our study, we screened 10 DEGs, which included *APOD*, *MASP1*, *ACKR1*, *C1QTNF7*, *SFRP4*, *HSPB6*, *GSTM5*, *IGFBP6*, *F10* and *DCN*, in cervical cancer tissues and paired adjacent normal tissues by RNA sequencing. All the expression levels of selected DEGs were down-regulated in tumors in both our clinical specimens and public database analysis. These genes showed great value in diagnosing the status of carcinogenesis. However, only the expression levels of *APOD*, *ACKR1* and *SFRP4* could predict the survival of patients. We are the first team to pay attention to the relationship between *C1QTNF7*, *HSPB6*, *GSTM5*, *IGFBP6*, *F10* and cervical cancer. Therefore, our results could provide novel candidate genes for future in-depth research on cervical tumorigenesis mechanisms and establishment of diagnostic or prognostic models.

ACKNOWLEDGEMENTS

ABBREVIATIONS

DEG	Differentially expressed gene
NGS	Next-generation sequencing
GO	Gene Ontology
DisGeNET	Disease Gene Network
KEGG	Kyoto Encyclopedia of Genes and Genomes
TCGA	The Cancer Genome Atlas
GTEx	Genotype-Tissue Expression Project
ROC curve	Receiver operating characteristic curve
APOD	Apolipoprotein D
MASP1	Mannose-Binding Lectin-Associated Serine Protease 1
ACKR1	Atypical Chemokine Receptor 1
C1QTNF7	Complement C1q Tumor Necrosis Factor-Related Protein 7
SFRP4	Secreted Frizzled Related Protein 4
HSPB6	Heat Shock Protein Family B (Small) Member 6
GSTM5	Glutathione S-Transferase Mu 5
IGFBP6	Insulin Like Growth Factor Binding Protein 6
F10	Coagulation Factor X
DCN	Decorin
AUC	Area under the curve

HR-HPV	High-risk human papillomavirus
MEK	Mitogen-activated extracellular signal-regulated kinase
ERK	Extracellular signal-regulated kinase
PI3K	Phosphoinositide 3-kinase
AKT	Serine/Threonine Kinase
EGFR	Epidermal Growth Factor Receptor
VEGFR	Vascular Endothelial Growth Factor
NF-κB	Nuclear factor-kappaB
STAT1	Signal Transducer And Activator Of Transcription 1
IRF3	Interferon Regulatory Factor 3
IRF1	Interferon Regulatory Factor 1
MIP-3α	Macrophage inflammatory protein-3 alpha
HLA	Human leukocyte antigen
SCC-Ag	Squamous Cell Carcinoma Antigen
FIGO	International Federation of Gynecology and Obstetrics
RT-qPCR	Quantitative Real Time Polymerase Chain Reaction
OS	Overall survival
GAPDH	Glyceraldehyde-3-Phosphate Dehydrogenase
CC	Cellular component
MF	Molecular function
BP	Biological process
WHO	World Health Organization
GEPIA2	Gene Expression Profiling Interactive Analysis 2
DARC	Duffy antigen receptor for chemokines
CTRP7	C1q complement/TNF related protein 7
HSP	Heat shock proteins
ROS	Reactive oxygen species
IGF II	Insulin-Like Growth Factor II
PAR-1	Protease-activated receptor-1
LIMK	LIM Domain Kinase
Lnc-RNA	Long non-coding RNA
PGM5-AS1	PGM5 Antisense RNA 1

ADDITIONAL INFORMATION AND DECLARATIONS

Funding

Competing Interests
The authors declare that they have no competing interests.

Author Contributions
- Jia Xu conceived and designed the experiments, performed the experiments, analyzed the data, prepared figures and/or tables, authored or reviewed drafts of the article, and approved the final draft.
- Wen Yang conceived and designed the experiments, analyzed the data, authored or reviewed drafts of the article, and approved the final draft.
- Xiufeng Xie performed the experiments, prepared figures and/or tables, and approved the final draft.
- Chenglei Gu performed the experiments, prepared figures and/or tables, and approved the final draft.
- Luyang Zhao performed the experiments, prepared figures and/or tables, and approved the final draft.
- Feng Liu performed the experiments, prepared figures and/or tables, and approved the final draft.
- Nina Zhang performed the experiments, prepared figures and/or tables, and approved the final draft.
- Yuge Bai performed the experiments, prepared figures and/or tables, and approved the final draft.
- Dan Liu performed the experiments, prepared figures and/or tables, and approved the final draft.
- Hainan Liu performed the experiments, prepared figures and/or tables, and approved the final draft.
- Xiangshu Jin conceived and designed the experiments, authored or reviewed drafts of the article, and approved the final draft.
- Yuanguang Meng conceived and designed the experiments, authored or reviewed drafts of the article, and approved the final draft.

Human Ethics
The following information was supplied relating to ethical approvals (*i.e.*, approving body and any reference numbers):

All the specimens were obtained after approval from the Ethics Committee of Seventh Medical Center of Chinese PLA General Hospital (S2023-025-01) and written informed

consent was collected from patients in the Department of Obstetrics and Gynecology of the Seventh Medical Center of PLA General Hospital.

DNA Deposition

The following information was supplied regarding the deposition of DNA sequences:

The sequence data of this study are available at Gene Expression Omnibus (GEO): GSE253690.

Data Availability

The following information was supplied regarding data availability:

The sequence data of this study are available at Gene Expression Omnibus (GEO): GSE253690.

The data of public database analysis and RT-qPCR are available at figshare: Xu, Jia; Yang, Wen; Jin, Xiangshu; Meng, Yuanguang (2024). Raw data for paper "Identification of 10 differentially expressed genes in tumorigenesis of cervical cancer *via* next generation sequencing". zip.figshare. Dataset. https://doi.org/10.6084/m9.figshare.25249534.v1.

Supplemental Information

Supplemental information for this article can be found online at http://dx.doi.org/10.7717/peerj.18157#supplemental-information.

REFERENCES

Alemayehu D, Zou KH. 2012. Applications of ROC analysis in medical research: recent developments and future directions. *Academic Radiology* **19(12)**:1457–1464 DOI 10.1016/j.acra.2012.09.006.

Bach LA. 2015a. Insulin-like growth factor binding proteins 4–6. *Best Practice & Research Clinical Endocrinology & Metabolism* **29(5)**:713–722 DOI 10.1016/j.beem.2015.06.002.

Bach LA. 2015b. Recent insights into the actions of IGFBP-6. *Journal of Cell Communication and Signaling* **9(2)**:189–200 DOI 10.1007/s12079-015-0288-4.

Bach Leon A, Fu P, Yang Z. 2012. Insulin-like growth factor-binding protein-6 and cancer. *Clinical Science* **124(4)**:215–229 DOI 10.1042/CS20120343.

Bedell SL, Goldstein LS, Goldstein AR, Goldstein AT. 2020. Cervical cancer screening: past, present, and future. *Sexual Medicine Reviews* **8(1)**:28–37 DOI 10.1016/j.sxmr.2019.09.005.

Bei Y, Huang Q, Shen J, Shi J, Shen C, Xu P, Chang H, Xia X, Xu L, Ji B, Chen J. 2016. IGFBP6 regulates cell apoptosis and migration in Glioma. *Cellular and Molecular Neurobiology* **37(5)**:889–898 DOI 10.1007/s10571-016-0426-4.

Bi J, Duan Y, Wang M, He C, Li X, Zhang X, Tao Y, Du Y, Liu H. 2022. Deletion of large-conductance calcium-activated potassium channels promotes vascular remodelling through the CTRP7-mediated PI3K/Akt signaling pathway. *Acta Biochimica et Biophysica Sinica* **466**:875 DOI 10.3724/abbs.2022179.

Borensztajn K, Bijlsma MF, Reitsma PH, Peppelenbosch MP, Spek CA. 2009. Coagulation factor Xa inhibits cancer cell migration via protease-activated receptor-1 activation. *Thrombosis Research* **124(2)**:219–225 DOI 10.1016/j.thromres.2009.01.015.

Borensztajn K, Peppelenbosch MP, Spek CA. 2010. Coagulation factor Xa inhibits cancer cell migration via LIMK1-mediated cofilin inactivation. *Thrombosis Research* **125(6)**:e323–e328 DOI 10.1016/j.thromres.2010.02.018.

Bray F, Laversanne M, Sung H, Ferlay J, Siegel RL, Soerjomataram I, Jemal A. 2024. Global cancer statistics 2022: GLOBOCAN estimates of incidence and mortality worldwide for 36 cancers in 185 countries. *CA: A Cancer Journal for Clinicians* **74(3)**:229–263 DOI 10.3322/caac.21834.

Chen Y, Li B, Wang J, Liu J, Wang Z, Mao Y, Liu S, Liao X, Chen J. 2020. Identification and verification of the prognostic value of the glutathione S-transferase Mu genes in gastric cancer. *Oncology Letters* **20(4)**:100 DOI 10.3892/ol.2020.11961.

Chen Y, Xu T, Xie F, Wang L, Liang Z, Li D, Liang Y, Zhao K, Qi X, Yang X, Jiao W. 2021. Evaluating the biological functions of the prognostic genes identified by the pathology Atlas in bladder cancer. *Oncology Reports* **45(1)**:191–201 DOI 10.3892/or.2020.7853.

Chua MW, Lin MZ, Martin JL, Baxter RC. 2015. Involvement of the insulin-like growth factor binding proteins in the cancer cell response to DNA damage. *Journal of Cell Communication and Signaling* **9(2)**:167–176 DOI 10.1007/s12079-015-0262-1.

Chung M-T, Sytwu H-K, Yan M-D, Shih Y-L, Chang C-C, Yu M-H, Chu T-Y, Lai H-C, Lin Y-W. 2009. Promoter methylation of SFRPs gene family in cervical cancer. *Gynecologic Oncology* **112(2)**:301–306 DOI 10.1016/j.ygyno.2008.10.004.

Crawford KS, Volkman BF. 2023. Prospects for targeting ACKR1 in cancer and other diseases. *Frontiers in Immunology* **14**:3033 DOI 10.3389/fimmu.2023.1111960.

Edwards HV, Cameron RT, Baillie GS. 2011. The emerging role of HSP20 as a multifunctional protective agent. *Cell Signal* **23(9)**:1447–1454 DOI 10.1016/j.cellsig.2011.05.009.

Falanga A, Marchetti M, Vignoli A. 2013. Coagulation and cancer: biological and clinical aspects. *Journal of Thrombosis and Haemostasis* **11(2)**:223–233 DOI 10.1111/jth.12075.

Fan G, Chu G, Kranias E. 2005. Hsp20 and its cardioprotection. *Trends in Cardiovascular Medicine* **15(4)**:138–141 DOI 10.1016/j.tcm.2005.05.004.

Feng Y, Huang Z, Lu F, Song L, Liu R, Zhang Y, Li N, Han X, Li X, Li K, Huang B, Xie G, Guo A, Yang J, Jia Z. 2024. 8-Br-cGMP activates HSPB6 and increases the antineoplastic activity of quinidine in prostate cancer. *Cell Death Discovery* **10(1)**:90 DOI 10.1038/s41420-024-01853-3.

Flynn R. 2012. Survival analysis. *Journal of Clinical Nursing* **21(19 pt 20)**:2789–2797 DOI 10.1111/j.1365-2702.2011.04023.x.

Ghoshal A, Ghosh SS. 2016. Antagonizing canonical Wnt signaling pathway by recombinant human sFRP4 purified from E. coli and its implications in cancer therapy. *Molecular and Cellular Biochemistry* **418(1–2)**:119–135 DOI 10.1007/s11010-016-2738-6.

Graf C, Wilgenbus P, Pagel S, Pott J, Marini F, Reyda S, Kitano M, Macher-Göppinger S, Weiler H, Ruf W. 2019. Myeloid cell-synthesized coagulation factor X dampens antitumor immunity. *Science Immunology* **4(39)**:eaaw8405 DOI 10.1126/sciimmunol.aaw8405.

Groeneveld CS, Chagas VS, Jones SJM, Robertson AG, Ponder BAJ, Meyer KB, Castro MAA. 2019. RTNsurvival: an R/Bioconductor package for regulatory network survival analysis. *Bioinformatics* **35(21)**:4488–4489 DOI 10.1093/bioinformatics/btz229.

Guo L, Xiao K, Xie Y, Yang Z, Lei J, Cai L. 2023. Overexpression of HSPB6 inhibits osteosarcoma progress through the ERK signaling pathway. *Clinical and Experimental Medicine* **23(8)**:5389–5398 DOI 10.1007/s10238-023-01216-9.

Hao X, Zhang J, Chen G, Cao W, Chen H, Chen S. 2022. Aberrant expression of GSTM5 in lung adenocarcinoma is associated with DNA hypermethylation and poor prognosis. *BMC Cancer* **22(1)**:299 DOI 10.1186/s12885-022-09711-0.

Hou T, Liang D, Xu L, Huang X, Huang Y, Zhang Y. 2013. Atypical chemokine receptors predict lymph node metastasis and prognosis in patients with cervical squamous cell cancer. *Gynecologic Oncology* **130(1)**:181–187 DOI 10.1016/j.ygyno.2013.04.015.

Hu X, Villodre ES, Larson R, Rahal OM, Wang X, Gong Y, Song J, Krishnamurthy S, Ueno NT, Tripathy D, Woodward WA, Debeb BG. 2021b. Decorin-mediated suppression of tumorigenesis, invasion, and metastasis in inflammatory breast cancer. *Communications Biology* **4(1)**:423 DOI 10.1038/s42003-020-01590-0.

Hu W, Zhan B, Li Q, Yang G, Yang M, Tan M, Geng S, Liu H, Chen C, Liu D, Li L. 2021a. Circulating CTRP7 is a potential predictor for metabolic syndrome. *Frontiers in Endocrinology* **12**:e3085 DOI 10.3389/fendo.2021.774309.

Jiang P, Cao Y, Gao F, Sun W, Liu J, Ma Z, Xie M, Fu S. 2021. SNX10 and PTGDS are associated with the progression and prognosis of cervical squamous cell carcinoma. *BMC Cancer* **21(1)**:87 DOI 10.1186/s12885-021-08212-w.

Jin X, Li Y, Guo Y, Jia Y, Qu H, Lu Y, Song P, Zhang X, Shao Y, Qi D, Xu W, Quan C. 2019. ERalpha is required for suppressing OCT4-induced proliferation of breast cancer cells via DNMT1/ISL1/ERK axis. *Cell Proliferation* **52(4)**:e12612 DOI 10.1111/cpr.12612.

Jou Y-C, Wang S-C, Dia Y-C, Wang S-T, Yu M-H, Yang H-Y, Chen L-C, Shen C-H, Liu Y-W. 2021. Anti-cancer effects and tumor marker role of glutathione s-transferase Mu 5 in human bladder cancer. *International Journal of Molecular Sciences* **22(6)**:3056 DOI 10.3390/ijms22063056.

Ju YT, Kwag SJ, Park HJ, Jung EJ, Jeong CY, Jeong SH, Lee YJ, Choi SK, Kang KR, Hah YS, Hong SC. 2015. Decreased expression of heat shock protein 20 in colorectal cancer and its implication in tumorigenesis. *Journal of Cellular Biochemistry* **116(2)**:277–286 DOI 10.1002/jcb.24966.

Kong L, Wang J, Cheng J, Zang C, Chen F, Wang W, Zhao H, Wang Y, Wang D. 2020. Comprehensive identification of the human secretome as potential indicators in treatment outcome of HPV-positive and -negative cervical cancer patients. *Gynecologic and Obstetric Investigation* **85(5)**:405–415 DOI 10.1159/000510713.

Kusakabe M, Taguchi A, Sone K, Mori M, Osuga Y. 2023. Carcinogenesis and management of human papillomavirus-associated cervical cancer. *International Journal of Clinical Oncology* **28(8)**:965–974 DOI 10.1007/s10147-023-02337-7.

Lange S, Gonzalez I, Pinto MP, Arce M, Valenzuela R, Aranda E, Elliot M, Alvarez M, Henriquez S, Velasquez EV, Orge F, Oliva B, Gonzalez P, Villalon M, Cautivo KM, Kalergis AM, Pereira K, Mendoza C, Saez C, Kato S, Cuello MA, Parborell F, Irusta G, Palma V, Allende ML, Owen GI. 2014. Independent anti-angiogenic capacities of coagulation factors X and Xa. *Journal of Cellular Physiology* **229(11)**:1673–1680 DOI 10.1002/jcp.24612.

Lata S, Mishra R, Arya RP, Arora P, Lahon A, Banerjea AC, Sood V. 2022. Where all the roads meet? A crossover perspective on host factors regulating SARS-CoV-2 infection. *Journal of Molecular Biology* **434(5)**:167403 DOI 10.1016/j.jmb.2021.167403.

Li J, Feng X, Zhu C, Jiang Y, Liu H, Feng W, Lu H. 2023. Intact glycopeptides identified by LC-MS/MS as biomarkers for response to chemotherapy of locally advanced cervical cancer. *Frontiers in Oncology* **13**:394 DOI 10.3389/fonc.2023.1149599.

Liso A, Capitanio N, Gerli R, Conese M. 2018. From fever to immunity: a new role for IGFBP-6? *Journal of Cellular and Molecular Medicine* **22(10)**:4588–4596 DOI 10.1111/jcmm.13738.

Liu J, Li S, Lin L, Jiang Y, Wan Y, Zhou S, Cheng W. 2020. Co-expression network analysis identified atypical chemokine receptor 1 (ACKR1) association with lymph node metastasis and prognosis in cervical cancer. *Cancer Biomarkers* **27(2)**:213–223 DOI 10.3233/CBM-190533.

Liu J, Lichtenberg T, Hoadley KA, Poisson LM, Lazar AJ, Cherniack AD, Kovatich AJ, Benz CC, Levine DA, Lee AV, Omberg L, Wolf DM, Shriver CD, Thorsson V, Hu H, Caesar-Johnson SJ, Demchok JA, Felau I, Kasapi M, Ferguson ML, Hutter CM, Sofia HJ, Tarnuzzer R, Wang Z, Yang L, Zenklusen JC, Zhang J, Chudamani S, Liu J, Lolla L, Naresh R, Pihl T, Sun Q, Wan Y, Wu Y, Cho J, DeFreitas T, Frazer S, Gehlenborg N, Getz G, Heiman DI, Kim J, Lawrence MS, Lin P, Meier S, Noble MS, Saksena G, Voet D, Zhang H, Bernard B, Chambwe N, Dhankani V, Knijnenburg T, Kramer R, Leinonen K, Liu Y, Miller M, Reynolds S, Shmulevich I, Thorsson V, Zhang W, Akbani R, Broom BM, Hegde AM, Ju Z, Kanchi RS, Korkut A, Li J, Liang H, Ling S, Liu W, Lu Y, Mills GB, Ng K-S, Rao A, Ryan M, Wang J, Weinstein JN, Zhang J, Abeshouse A, Armenia J, Chakravarty D, Chatila WK, de Bruijn I, Gao J, Gross BE, Heins ZJ, Kundra R, La K, Ladanyi M, Luna A, Nissan MG, Ochoa A, Phillips SM, Reznik E, Sanchez-Vega F, Sander C, Schultz N, Sheridan R, Sumer SO, Sun Y, Taylor BS, Wang J, Zhang H, Anur P, Peto M, Spellman P, Benz C, Stuart JM, Wong CK, Yau C, Hayes DN, Parker JS, Wilkerson MD, Ally A, Balasundaram M, Bowlby R, Brooks D, Carlsen R, Chuah E, Dhalla N, Holt R, Jones SJM, Kasaian K, Lee D, Ma Y, Marra MA, Mayo M, Moore RA, Mungall AJ, Mungall K, Robertson AG, Sadeghi S, Schein JE, Sipahimalani P, Tam A, Thiessen N, Tse K, Wong T, Berger AC, Beroukhim R, Cherniack AD, Cibulskis C, Gabriel SB, Gao GF, Ha G, Meyerson M, Schumacher SE, Shih J, Kucherlapati MH, Kucherlapati RS, Baylin S, Cope L, Danilova L, Bootwalla MS, Lai PH, Maglinte DT, Van Den Berg DJ, Weisenberger DJ, Auman JT, Balu S, Bodenheimer T, Fan C, Hoadley KA, Hoyle AP, Jefferys SR, Jones CD, Meng S, Mieczkowski PA, Mose LE, Perou AH, Perou CM, Roach J, Shi Y, Simons JV, Skelly T, Soloway MG, Tan D, Veluvolu U, Fan H, Hinoue T, Laird PW, Shen H, Zhou W, Bellair M, Chang K, Covington K, Creighton CJ, Dinh H, Doddapaneni H, Donehower LA, Drummond J, Gibbs RA, Glenn R, Hale W, Han Y, Hu J, Korchina V, Lee S, Lewis L, et al. 2018. An integrated TCGA Pan-cancer clinical data resource to drive high-quality survival outcome analytics. *Cell* **173(2)**:400–416.e411 DOI 10.1016/j.cell.2018.02.052.

Liu J, Zhu S, Zeng L, Li J, Klionsky DJ, Kroemer G, Jiang J, Tang D, Kang R. 2021. DCN released from ferroptotic cells ignites AGER-dependent immune responses. *Autophagy* **18(9)**:2036–2049 DOI 10.1080/15548627.2021.2008692.

Love MI, Huber W, Anders S. 2014. Moderated estimation of fold change and dispersion for RNA-seq data with DESeq2. *Genome Biology* **15(12)**:550 DOI 10.1186/s13059-014-0550-8.

Maestri CA, Nisihara R, Mendes HW, Jensenius J, Thiel S, Messias-Reason I, de Carvalho NS. 2018. MASP-1 and MASP-2 serum levels are associated with worse prognostic in cervical cancer progression. *Frontiers in Immunology* **9**:2742 DOI 10.3389/fimmu.2018.02742.

Manzo-Merino J, Contreras-Paredes A, Vazquez-Ulloa E, Rocha-Zavaleta L, Fuentes-Gonzalez AM, Lizano M. 2014. The role of signaling pathways in cervical cancer and molecular therapeutic targets. *Archives of Medical Research* **45(7)**:525–539 DOI 10.1016/j.arcmed.2014.10.008.

Matsushima-Nishiwaki R, Toyoda H, Nagasawa T, Yasuda E, Chiba N, Okuda S, Maeda A, Kaneoka Y, Kumada T, Kozawa O. 2016. Phosphorylated heat shock protein 20 (HSPB6) regulates transforming growth factor-alpha-induced migration and invasion of hepatocellular carcinoma cells. *PLOS ONE* **11(4)**:e0151907 DOI 10.1371/journal.pone.0151907.

Matsushita M, Endo Y, Fujita T. 1998. MASP1 (MBL-associated serine protease 1). *Immunobiology* **199(2)**:340–347 DOI 10.1016/s0171-2985(98)80038-7.

Nagasawa T, Matsushima-Nishiwaki R, Toyoda H, Matsuura J, Kumada T, Kozawa O. 2014. Heat shock protein 20 (HSPB6) regulates apoptosis in human hepatocellular carcinoma cells: direct association with Bax. *Oncology Reports* **32(3)**:1291–1295 DOI 10.3892/or.2014.3278.

Nagelhout G, Ebisch RM, Van Der Hel O, Meerkerk GJ, Magnee T, De Bruijn T, Van Straaten B. 2021. Is smoking an independent risk factor for developing cervical intra-epithelial neoplasia and cervical cancer? A systematic review and meta-analysis. *Expert Review of Anticancer Therapy* **21(7)**:781–794 DOI 10.1080/14737140.2021.1888719.

Narisawa-Saito M, Kiyono T. 2007. Basic mechanisms of high-risk human papillomavirus-induced carcinogenesis: roles of E6 and E7 proteins. *Cancer Science* **98(10)**:1505–1511 DOI 10.1111/j.1349-7006.2007.00546.x.

Nikulin S, Razumovskaya A, Poloznikov A, Zakharova G, Alekseev B, Tonevitsky A. 2023. ELOVL5 and IGFBP6 genes modulate sensitivity of breast cancer cells to ferroptosis. *Frontiers in Molecular Biosciences* **10**:1075704 DOI 10.3389/fmolb.2023.1075704.

Nikulin S, Zakharova G, Poloznikov A, Raigorodskaya M, Wicklein D, Schumacher U, Nersisyan S, Bergquist J, Bakalkin G, Astakhova L, Tonevitsky A. 2021. Effect of the expression of ELOVL5 and IGFBP6 genes on the metastatic potential of breast cancer cells. *Frontiers in Genetics* **12**:662843 DOI 10.3389/fgene.2021.662843.

Obuchowski NA, Bullen JA. 2018. Receiver operating characteristic (ROC) curves: review of methods with applications in diagnostic medicine. *Physics in Medicine & Biology* **63(7)**:07TR01 DOI 10.1088/1361-6560/aab4b1.

Pawar NM, Rao P. 2018. Secreted frizzled related protein 4 (sFRP4) update: a brief review. *Cellular Signalling* **45(8)**:63–70 DOI 10.1016/j.cellsig.2018.01.019.

Peng DF, Razvi M, Chen H, Washington K, Roessner A, Schneider-Stock R, El-Rifai W. 2008. DNA hypermethylation regulates the expression of members of the Mu-class glutathione S-transferases and glutathione peroxidases in Barrett's adenocarcinoma. *Gut* **58(1)**:5–15 DOI 10.1136/gut.2007.146290.

Petersen PS, Lei X, Wolf RM, Rodriguez S, Tan SY, Little HC, Schweitzer MA, Magnuson TH, Steele KE, Wong GW. 2017. CTRP7 deletion attenuates obesity-linked glucose intolerance, adipose tissue inflammation, and hepatic stress. *American Journal of Physiology-Endocrinology and Metabolism* **312(4)**:E309–E325 DOI 10.1152/ajpendo.00344.2016.

Rassart E, Desmarais F, Najyb O, Bergeron K-F, Mounier C. 2020. Apolipoprotein D. *Gene* **756(1)**:144874 DOI 10.1016/j.gene.2020.144874.

Robin X, Turck N, Hainard A, Tiberti N, Lisacek F, Sanchez JC, Muller M. 2011. pROC: an open-source package for R and S+ to analyze and compare ROC curves. *BMC Bioinformatics* **12(1)**:77 DOI 10.1186/1471-2105-12-77.

Robinson MD, McCarthy DJ, Smyth GK. 2010. edgeR: a bioconductor package for differential expression analysis of digital gene expression data. *Bioinformatics* **26(1)**:139–140 DOI 10.1093/bioinformatics/btp616.

Salvo G, Ramirez PT, Leitao MM, Cibula D, Wu X, Falconer H, Persson J, Perrotta M, Mosgaard BJ, Kucukmetin A, Berlev I, Rendon G, Liu K, Vieira M, Capilna ME, Fotopoulou C, Baiocchi G, Kaidarova D, Ribeiro R, Pedra-Nobre S, Kocian R, Li X, Li J, Pálsdóttir K, Noll F, Rundle S, Ulrikh E, Hu Z, Gheorghe M, Saso S, Bolatbekova R, Tsunoda A, Pitcher B, Wu J, Urbauer D, Pareja R. 2022. Open vs minimally invasive radical trachelectomy in early-stage cervical cancer: international radical trachelectomy assessment study. *American Journal of Obstetrics and Gynecology* **226(1)**:97.e1–97.e16 DOI 10.1016/j.ajog.2021.08.029.

Shen CH, Li PY, Wang SC, Wu SR, Hsieh CY, Dai YC, Liu YW. 2023. Epigenetic regulation of human WIF1 and DNA methylation situation of WIF1 and GSTM5 in urothelial carcinoma. *Heliyon* **9(5)**:e16004 DOI 10.1016/j.heliyon.2023.e16004.

Siegel RL, Miller KD, Wagle NS, Jemal A. 2023. Cancer statistics, 2023. *CA: A Cancer Journal for Clinicians* **73(1)**:17–48 DOI 10.3322/caac.21763.

Song JY, Lee JK, Lee NW, Jung HH, Kim SH, Lee KW. 2008. Microarray analysis of normal cervix, carcinoma in situ, and invasive cervical cancer: identification of candidate genes in pathogenesis of invasion in cervical cancer. *International Journal of Gynecologic Cancer* **18(5)**:1051–1059 DOI 10.1111/j.1525-1438.2007.01164.x.

Vivian J, Rao AA, Nothaft FA, Ketchum C, Armstrong J, Novak A, Pfeil J, Narkizian J, Deran AD, Musselman-Brown A, Schmidt H, Amstutz P, Craft B, Goldman M, Rosenbloom K, Cline M, O'Connor B, Hanna M, Birger C, Kent WJ, Patterson DA, Joseph AD, Zhu J, Zaranek S, Getz G, Haussler D, Paten B. 2017. Toil enables reproducible, open source, big biomedical data analyses. *Nature Biotechnology* **35(4)**:314–316 DOI 10.1038/nbt.3772.

Volkova LV, Pashov AI, Omelchuk NN. 2021. Cervical carcinoma: oncobiology and biomarkers. *International Journal of Molecular Sciences* **22(22)**:12571 DOI 10.3390/ijms222212571.

Wang L, Deng Z, Yang J, Zhao Y, Zhou L, Diao L, Li L, Cheng Y. 2022b. Epigenetic and transcriptomic characterization of maternal-fetal interface in patients with recurrent miscarriage via an integrated multi-omics approach. *Journal of Reproductive Immunology* **154**:103754 DOI 10.1016/j.jri.2022.103754.

Wang Q, Vattai A, Vilsmaier T, Kaltofen T, Steger A, Mayr D, Mahner S, Jeschke U, Heidegger HH. 2021. Immunogenomic identification for predicting the prognosis of cervical cancer patients. *International Journal of Molecular Sciences* **22(5)**:2442 DOI 10.3390/ijms22052442.

Wang H, Wang D, Wei Q, Li C, Li C, Yang J. 2022a. Long non-coding RNAs PGM5-AS1 upregulates Decorin (DCN) to inhibit cervical cancer progression by sponging miR-4284. *Bioengineered* **13(4)**:9872–9884 DOI 10.1080/21655979.2022.2062088.

Wong GW, Krawczyk SA, Kitidis-Mitrokostas C, Revett T, Gimeno R, Lodish HF. 2008. Molecular, biochemical and functional characterizations of C1q/TNF family members: adipose-tissue-selective expression patterns, regulation by PPAR-gamma agonist, cysteine-mediated oligomerizations, combinatorial associations and metabolic functions. *Biochemical Journal* **416(2)**:161–177 DOI 10.1042/BJ20081240.

Wu Y, Zhao J, Tian Y, Jin H. 2023. Cellular functions of heat shock protein 20 (HSPB6) in cancer: a review. *Cellular Signalling* **112(7)**:110928 DOI 10.1016/j.cellsig.2023.110928.

Wyciszkiewicz A, Lach MS, Wroblewska JP, Michalak M, Suchorska WM, Kalinowska A, Michalak S. 2021. The involvement of small heat shock protein in chemoresistance in ovarian cancer—in vitro study. *EXCLI Journal* **20**:935–947 DOI 10.17179/excli2021-3706.

Xue S, Ling J, Tian M, Li K, Li S, Liu D, Li L, Yang M, Yang G. 2024. Combined serum CTRP7 and CTRP15 levels as a novel biomarker for insulin resistance and type 2 diabetes mellitus. *Heliyon* **10(9)**:e30029 DOI 10.1016/j.heliyon.2024.e30029.

Yang Y, Wu Y, Hou L, Ge X, Song G, Jin H. 2022. Heat shock protein 20 suppresses breast carcinogenesis by inhibiting the MAPK and AKT signaling pathways. *Oncology Letters* **24(6)**:462 DOI 10.3892/ol.2022.13582.

Yu G, Wang LG, Han Y, He QY. 2012. clusterProfiler: an R package for comparing biological themes among gene clusters. *Omics a Journal of Integrative Biology* **16(5)**:284–287 DOI 10.1089/omi.2011.0118.

Zhang H, Chen R, Shao J. 2020. MicroRNA-96-5p facilitates the viability, migration, and invasion and suppresses the apoptosis of cervical cancer cells by negatively modulating SFRP4.

Xu et al. (2024), *PeerJ*, DOI 10.7717/peerj.18157

28/29

Technology in Cancer Research & Treatment **19(3)**:153303382093413
DOI 10.1177/1533033820934132.

Zhang J, Li Y, Zou J, Lai CT, Zeng T, Peng J, Zou WD, Cao B, Liu D, Zhu LY, Li H, Li YK. 2022a. Comprehensive analysis of the glutathione S-transferase Mu (GSTM) gene family in ovarian cancer identifies prognostic and expression significance. *Frontiers in Oncology* **12**:968547 DOI 10.3389/fonc.2022.968547.

Zhang Y, Qin Y, Li D, Yang Y. 2022c. A risk prediction model mediated by genes of APOD/APOC1/SQLE associates with prognosis in cervical cancer. *BMC Women's Health* **22(1)**:2022 DOI 10.1186/s12905-022-02083-4.

Zhang W, Wang H, Qi Y, Li S, Geng C. 2022b. Epigenetic study of early breast cancer (EBC) based on DNA methylation and gene integration analysis. *Scientific Reports* **12(1)**:1989 DOI 10.1038/s41598-022-05486-3.

Zhao L, Gu C, Ye M, Zhang Z, Li L, Fan W, Meng Y. 2018. Integration analysis of microRNA and mRNA paired expression profiling identifies deregulated microRNA-transcription factor-gene regulatory networks in ovarian endometriosis. *Reproductive Biology and Endocrinology* **16(1)**:4 DOI 10.1186/s12958-017-0319-5.

Zhao C, Zhu X, Wang G, Wang W, Ju S, Wang X. 2020. Decreased expression of IGFBP6 correlates with poor survival in colorectal cancer patients. *Pathology Research and Practice* **216(5)**:152909 DOI 10.1016/j.prp.2020.152909.